ECN-77

ECN-77

ECN

OCTOBER 1979

A REACTOR STUDY ON A BELT-SHAPED SCREW PINCH

BY

M. BUSTRAAN[1], B. BRANDT[2], G.C. DAMSTRA[3], W.M.P. FRANKEN[1],

J.A. HOEKZEMA[2], H.J. KLEIN NIBBELINK[3], H.Th. KLIPPEL[1],

W. SCHUURMAN[2], H.J. VERINGA[1] AND K.A. VERSCHUUR[1].

also published as
Rijnhuizen Report 79 – 118

Netherlands Energy Research Foundation

Netherlands Energy Research Foundation ECN

P.O. Box 1

1755 ZG Petten (NH)

The Netherlands

Telephone (0)2246 - 6262

Telex 57211

ECN-77

OCTOBER 1979

A REACTOR STUDY ON A BELT-SHAPED SCREW PINCH

BY

M. BUSTRAAN[1], B. BRANDT[2], G.C. DAMSTRA[3], W.M.P. FRANKEN[1],

J.A. HOEKZEMA[2], H.J. KLEIN NIBBELINK[3], H.Th. KLIPPEL[1],

W. SCHUURMAN[2], K.J. VERINGA[1] AND K.A. VERSCHUUR[1].

also published as
Rijnhuizen Report 79 - 118

[1] ECN, Netherlands Energy Research Foundation, Petten.

[2] FOM Institute for Plasma Physics, Rijnhuizen, Jutphaas.

[3] KEMA, Arnhem.

M. Bustraan, B Brandt, G.C. Damstra, W.M.P. Franken, J.A. Hoekzema, H.J. Klein Nibbelink, H.Th. Klippel, W. Schuurman, H.J. Veringa and K.A. Verschuur.

A REACTOR STUDY ON A BELT-SHAPED SCREW PINCH.

Netherlands Energy Research Foundation (ECN), 1979, October
51 pages, 5 tables, 16 figures.

A previous study on a screw-pinch reactor with circular cross-section |ECN-16 (1977) or Rijnhuizen report 77-101| has been extended to a belt configuration which allows to raise β to 0.5. The present study starts from the main assumptions and principal constraints of the previous work, but some technical aspects are treated more realistically. More attention has been paid to the modular construction, the non-uniform distribution of the wall loading, the thermo-hydraulics, the design of and the losses in the coil systems, and the energy storage and electric transmission systems. A potential use of the first wall of the blanket as part of the implosion coil system is suggested. Finally, a conceptual design of a reactor, with a cost estimate is given. Numerical results are given of parameter variations around the values for the reference reactor. The belt screw-pinch reactor with resistive coils turns out to be uneconomical, because of its low net efficiency and its high capital costs. The application of superconducting coils to reduce the ohmic losses turns out to be a not viable alternative. A more promising way to improve the energy balance seems to be the alternative scheme of fuel injection during the burn.

KEYWORDS:

TOROIDAL SCREW PINCH DEVICES
BELT PINCH
CONSTRUCTION
HYDRAULICS
PLANNING
ENERGY STORAGE
ECONOMICS
ADIABATIC COMPRESSION HEATING
SHOCK HEATING
PULSED D-T REACTORS
PLASMA SIMULATION
WALL LOADING
HIGH-BETA PLASMA
PULSED MAGNET COILS
SUPERCONDUCTING MAGNETS
FUEL PELLETS
ABLATION
ACCELERATION

CONTENTS

This work was performed by a reactor study group in which FOM, RCN, and KEMA participate. It constitutes part of the research programme of the association agreement of Euratom and the "Stichting voor Fundamenteel Onderzoek der Materie" (FOM) with financial support from the "Nederlandse Organisatie voor Zuiver-Wetenschappelijk Onderzoek" (ZWO) and Euratom.

1. INTRODUCTION

Since 1975 work by the authors on system studies of pulsed high-beta fusion reactors is in progress. In view of the screw-pinch programme, based on the SPICA experiments |1|, special attention is given to the reactor potentialities of the screw-pinch configuration. A parameter study of a screw-pinch reactor with circular cross-section was presented at the 9th SOFT |2|, and later published in more detail in |3|. That study demonstrated the inefficiency of heating a plasma by adiabatic compression at β-values around 0.25. Recent theoretical investigations of ideal MHD-equilibrium and stability of screw-pinch columns |4| underline the considerable gain in β obtainable with elongated cross-sections. This encouraged the authors to extend the reactor study to a belt-shaped screw pinch with β around 0.5. The objectives of the present work are two-fold. Firstly, the earlier parameter study is extended to a belt geometry in order to find the improvements due to the higher β. Secondly, some technical aspects, a part of them related to the change in geometry, are treated more realistically in the present study. In the physical model (see section 2) the implosion has been treated quasi-twodimensional. Effects that have been taken account of in technology (section 3) are the non-uniform current of neutrons towards the first wall, the pumping power for the primary cooling circuit and the losses in the transmission systems of the implosion and compression circuits. In section 4 the parameters of the reference belt screw-pinch reactor (BSPR) are presented, the effects of some parameter variations are shown, and a cost evaluation is given.
Section 5 deals with the problems associated with the application of pulsed superconducting coils for the fast rising magnetic fields.
In section 6 the idea of fuel injection as a possible means to improve the net efficiency of the reactor is introduced. Finally, the general conclusions from this work are formulated in section 7.
A preliminary version of this study has been presented at the 10th SOFT conference.

2. PHYSICAL MODEL

A detailed description of the model is given in [5]. Here only a short survey is given.

After pre-ionization the 50-50% D-T mixture is heated by fast implosion. An initial bias field is applied to reduce β. This bias field B_o can be either normal (i.e. generated by a current in the compression coil, while discharge of a capacitor bank over the implosion coil effects the implosion) or sustained (the magnetic field generated by a current in the compression coil rises above the value B_o and is then sharply decreased to B_o by a current in the implosion coil), see Fig. 1.
In the calculations presented in this report the bias field has been taken normal, since for this case the initial field rise is faster and thus the implosion more effective. The time history of the magnetic field is shown in Fig. 2. In the implosion model the plasma and the initial bias field are swept up together in an imploding current sheath. Since the rise time of the magnetic field has to be short compared to the implosion time, the curvature of the plasma sheath during this rise time may be neglected. The basic assumption made in the calculation of inductances is that the distance between the plasma and the first wall is the same along the poloidal circumference (during implosion this assumption is reasonable and at a later stage it looses its importance). The time-dependent momentum equation for the plasma sheath, together with the equations for the TF implosion and compression circuits are solved numerically. The poloidal magnetic field is applied in such a way that q at the first wall is constant in time. The charging voltage of the capacitor bank (a free parameter) is iterated until the maximum value of the electric field strength at the first wall during the implosion takes on the maximum permissable value $\hat{E}_{wm}$.

It is assumed that after equilibration and thermalization, as well as during the burn, the plasma has a homogeneous pressure. The central plasma is surrounded by a force-free magnetic field with q = const.
The plasma is further heated to ignition by adiabatic compression, causing a lower β-value of the plasma. The burning phase consists of three stages (see Fig. 2). In the first stage the plasma is heated by α-particles and the magnetic field, that was necessarily high to reach

ignition, is reduced to its optimum value. When β approaches its maximum value β_{max}, high-Z impurities are injected to raise the radiation transfer to the first wall temporally to the level of the fusion power production. In the second stage, where β has become equal to β_{max}, thermal equilibrium is maintained at $\beta = \beta_{max}$ by active magnetic field control. In the third and final stage of the burn, when the required optimal amount of fusion energy has been produced, the plasma is allowed to cool down.

The adiabatic compression phase and the burn phase are described by zero-dimensional time-dependent equations for the particle balance, the pressure balance, and the energy balance.

In the overall power balance the losses include: ohmic losses in the resistive coils and in the transmission systems to the ETS, switching losses in the ETS-system, all the implosion bank energy, and the fraction of the poloidal field energy within the coil, that probably can not be recovered. In the earlier calculation of a screw-pinch reactor with circular cross-section the last-mentioned loss was not included, neither were the losses in the transmission systems; therefore the net efficiency found there was too optimistic.

3. TECHNICAL ASPECTS

3.1. Reference Belt Screw-Pinch Reactor

With the exception of the belt shape and the aspect ratio, the parameters determining the size of the reactor have been given the same values as for the circular screw-pinch reactor |3|. Comparison of both reactors will reveal the improvements and consequences resulting from the choice of the belt shape and of the more elaborated technical constraints. For the height-over-width ratio of the belt-shaped torus the value e=3 has been taken |4|.
With a thermal efficiency of $\eta_{th} = 0.42$ and an energy multiplication factor in the blanket of $Q_m = 1.2$, the thermal output $P_{th} = 6$ GW results in a gross electric output of $P_{gross} = 2.5$ GW. The torus dimensions (R = 10 m, 2b = 5 m, 2h = 15 m) and other parameters resulting from the calculations (see section 4) are given in table 1.

3.2. First-Wall Loading

Neutron transport calculations reveal that the elongated cross-section, the high plasma compression, the outward shift of the plasma column, and the small aspect ratio give rise to a pronounced non-uniformity in the poloidal distribution of the wall loading |6|. Some results for the reference reactor (averaged over the cycle time) are given in table 2. An average wall loading of $P_w = 2$ MW/m^2 results in a maximum wall loading of 5.3 MW/m^2. This non-uniformity influences the design of the blanket and its cooling. These values are in accordance with the general view that high wall loads are essential for economic fusion power plants. For Tokamak plants it has been shown that integral neutron wall loadings of 10 - 20 MWyr/m^2 and average neutron wall loadings of > 4 MW/m^2 are required to generate electricity at relatively low costs |7|. This calls for advanced radiation-resistant materials for the construction of at least the most heavily loaded parts of the first wall of our BSPR design. For such materials the life time of the first wall of the BSPR can be estimated at approximately 2 years. Due to the flattening of the neutron flux inside the blanket the variation of the power production in the blanket is smaller than that of the wall loading (as indicated by the values of table 2).

3.3. Blanket System

Stagnant lithium is assumed as breeder material, and a steel reflector is added to improve the breeding. As in the previous study, helium is chosen as blanket coolant. The poor accessibility of the inner blanket suggests to keept this part of the blanket non-breeding. In order to limit a consequential reduction of the breeding to about 20%, the neutron reflectivity of the inner blanket can be enhanced, e.g. by placing graphite in the inner modules, and by optimization of the remaining blanket. Accordingly, a blanket thickness d_b of 0.80 m is taken.

During the implosion phase an electric field of 3 kV/cm is generated at the first wall, resulting in a high voltage between adjacent blanket modules. Assuming 100 kV to be manageable electrotechnically, the lateral dimensions of the modules become 0.5×0.5 m^2 and the thickness of the insulating layer, covering each blanket module to withstand the voltage, has to be about 0.5 cm. The 10 000 modules of about 0.25 tons each, are supported by a vertical structure behind the blanket. This structure also contains the helium coolant ducts. Electrical conducting connections between the blanket modules are not allowed and therefore the modules have to be connected to the support structure and the coolant ducts by insulating ceramic joints. For these load bearing joints materials with good mechanical properties are required. For a number of ceramic insulating materials, information on such properties for use in fusion reactors is available [8]. With respect to the mechanical, electrical, thermal, and vacuum properties the silicon carbides seem to be suitable materials.

For the thin insulating layer covering the blanket modules important properties such as the irradiation behaviour, the high voltage insulation, and the surface effects are essential; however, sufficient information is lacking.
Also the part of the insulating layer facing the plasma is subject to high thermal stresses and fast neutron irradiation, therefore detachment of this layer from the structural wall might occur. However, the problems associated with these insulating layers have not been studied further. Smaller modules than selected here would be profitable with respect to the electric field and to module weight, the selected

size is a copromise between the technical aspects and the condition of a stable plasma during the burn.

3.4. Power Conversion System

The helium flow rate to each blanket module has to be adjusted to the non-uniform power production; the average power production per module is 600 kW, with a maximum of 1350 kW, and a minimum of 210 kW (see table 2). In this study a power conversion system consisting of a primary helium coolant circuit with a modest helium outlet temperature (650°C) combined with a steam-turbine generator circuit at high temperature has been chosen. In this case no special high-temperature materials have to be used for the cooling system and normal or high-grade steels may be applied.

The obvious thermodynamic advantages of operating at higher temperatures may be offset by the higher costs of the special materials required. It appears [9] that the selected power conversion system might be economically more attractive and less complicated than an advanced high-temperature reactor plant utilizing a closed-cycle helium gas turbine.

A thermo-hydraulic analysis of the system has been performed with an assumed helium temperature of 250°C at the inlet and of 650°C at the outlet of the modules, a maximum helium pressure of 50 bar, and a total relative pressure loss of 5%. This pressure drop of 2.5 bar resulting in an ideal pumping power of 150 MW, is a compromise between increasing investment costs (of the primary circuit and heat exchangers) and increasing cycle efficiency with decreasing pumping power.

In the analysis we assume that the pressure losses are equally divided over the blanket modules, the piping, and the heat exchangers.

Similar to the coil system the blanket is subdivided into 24 toroidal sections. Each of these sections needs separate coolant ducts for the outer, inner, upper, and lower blanket which are located directly behind the blanket modules. In the calculations all these ducts, the ring-shaped collectors for hot and cold helium, and the main ducts to the heat exchangers are assumed to have an equal pressure drop of 0.1 bar. The resulting diameters for the headers of each toroidal blanket section are: 0.45 m for the outer blanket, and 0.30 m for the inner, the upper, and the lower blanket.

The main ducts to the heat exchangers will be 2 m in diameter. The space behind the outer blanket occupied by the coolant ducts determines the distance between the blanket and the toroidal field coils, for which we find 0.5 m as a reasonable value.
In the calculations the power distribution in the blanket as given in section 2.2 is taken into account. One blanket module of the outer blanket, with an average wall loading of 2.8 MW/m^2, can be cooled by 40 m coolant channels of 0.01 m inner diameter, occupying about 2% of the blanket volume.
The blanket and the primary coolant system together have a thermal time constant of about 50 s. Therefore, the total heat capacity of the blanket, the primary coolant system, and the water-steam secondary circuit will smooth the temperature variation due to the periodically fluctuating power production. For the steam-turbine secondary system with an inlet temperature of about 600°C, a thermal efficiency of $\eta_{th} = 42\%$ is expected.
The helium circulators are assumed to be driven electrically. The ideal pumping power is 150 MW. Assuming an isentropic efficiency of 88% and mechanical and electrical losses of 10 MW, the electrical power supplied to the helium circulators will be 180 MW, of which the convertible enthalpy rise of the helium (= 170 MW) is taken into account in the overall energy balance. Fig. 3 shows the energy flow diagram of the reference reactor. Two steam turbine generator units of nominal 1200 MW each are envisaged. One of them supplies electric energy at fixed frequency to the grid and the helium circulators, the other feeds the electric systems of the reactor, e.g. the homopolar generators and the capacitor banks, at a frequency depending on the periodically varying load.

3.5. Implosion Coil System

The implosion circuit must deliver a fast rising magnetic field. Penetration of this magnetic field requires separating slits between the blanket modules, both in toroidal and poloidal directions. A single turn implosion coild would need a total voltage of 12 MV, to be fed by storage capacitors. Since these have a limited maximum voltage the single turn has to be subdivided into segments. This suggests to use

the first wall of the blanket modules directly as the segments of the implosion coil. The required screw configuration of the magnetic field is obtained by connecting the modules in an appropriate pattern.
The storage bank will be subdivided into 10 000 units, each feeding one of the modules acting now as a coil segment. This requires a complicated transmission system. The average distance between modules and storage capacitors is about 15 m. Therefore, the inductance of the transmission system adds substantially to that of the capacitor banks, resulting in the required storage energy of 940 MJ and a voltage of 300 kV per storage unit. The latter requirement aggravates the technological problems considerably.
For systems on a reactor scale, the ratio of the circuit inductance to the plasma inductance proves to be a critical parameter. The 940 MJ storage capacitors together have a volume of 24000 m^3 and a weight of 20 000 tons. The average power needed to recharge the banks is 40 MW.

3.6. Compression Coil System

To avoid the problems of helical coils, separate innerlying toroidal field (TF) and outerlying poloidal field (PF) coild have been used for the compression system. The upper yokes of the rectangular TF-coils are thought to be demountable for vertical access to the blanket.
The data of the coils are given in tables 1 and 3. A compromise between ohmic losses and weight (see section 4.2.) leads to a total copper weight of 38 000 tons.
The coils are watercooled at 60°C temperature. The maximum current density in the coils is 3.5 MA/m^2. The compression energy (W_{TF} = 94 GJ, W_{PF} = 17 GJ) is stored periodically in 288 homopolar machines of about 0.5 GJ each (1 MA, 8 kV). For the transfer efficiency η_{ets} of this circuit, in ref. [3] assumed to be 98%, the more realistic value of 95% has now been taken [10].
An analysis revealed that the average tensile stresses in the coil material are well within the allowable limits, However, the bending forces, as a result of the rectangular shape, would require a huge restraining construction. It has not been studied how far a more realistic D-shape of the coils would be more profitable.
The homopolar machines are installed around the reactor at an average

distance of 7.5 meter. The corresponding transmission system is segmented in 288 radial water-cooled busbars carrying 1 MA each. The power loss in such busbars is 90 kW/m, giving a total power loss of 200 MW in the transmission system. The busbars have a total copper weight of 9000 tons. To compensate for the losses an average power of 1190 MW is supplied to the homopolar machines during the down time.

3.7. Design Considerations and General Station Lay-out

Due to the low aspect ratio the access to the inner blanket is difficult. This problem is aggravated by the large space occupied by the coils. The implosion heating mechanism forbids the presence of a closed conducting first wall, therefore the closed metallic vacuum-tight wall has to be situated outside the magnetic coils. This vacuum wall is placed against a supporting concrete wall just outside the coils. These walls together act as the outside reactor vessel. The energy storage systems are located outside this reactor vessel, as close to the coils as possible, so that the transmission losses will be minimal.
The presence of these large storage systems around the reactor vessel makes horizontal access to the blanket impossible. Access is vertically through the narrow space between the coils, and can be improved by the use of demountable upper yokes on the coils.
Two independent vacuum pumping systems are envisaged: one high-vacuum system with an intensive tritium purification for the plasma torus and a second lower-vacuum system with less tritium purification for the remaining space in the reactor vessel.
To remove the unburned fuel and the ash during the down time a pumping rate of 4000 m^3/s at 60 MW is required. Per toroidal section, two vacuum ducts of 1.5 m diameter are needed. These ducts enter the torus in the upper and lower corners of the outer blanket, where leakage of neutrons will be small,
The first wall, the blanket, the coils inside the reactor vessel, and the energy storage systems outside the reactor vessel constitute a very tightly packed and massive structure within a leaktight outer containment. The dimensions, weights, and global capital costs derived from the reference parameters are given in table 3. Figure 3 gives the energy-flow diagram, and figure 4 gives a general impression of a possible station lay-out.

4. REACTOR PARAMETER STUDY

4.1. Numerical Calculations

The optimal reactor parameters are found in essentially the same way as for the reactor with circular cross-section [3]. Again the plasma is heated to ignition by fast implosion and subsequent adiabatic compression. During the burn phase the plasma is kept in thermal equilibrium by addition of impurities and by magnetic field control. The numerical program solves the time-dependent equations. The block diagram of this program is given in figure 5. Some differences in the calculations compared to those for the circular cross-section are as follows.
The poloidal fields become more important for higher ellipticity and therefore are now included in the calculations. In the implosion model the plasma and the initial bias field are swept up together in an imploding current sheath. The broadening of this sheath is approximately taken into account [11]
In the overall power balance the losses include ohmic losses in the normally conducting resistive coils and in the transmission systems to the ETS, switching losses of the ETS-system, all the implosion bank energy, and the fraction of the poloidal field energy within the coils that can probably not be recovered.
In the most unfavourable case the burn has to be quenched before the energy can be transferred to the ETS-system. In that case the poloidal field energy inside the PF-coil plus the major part of the energy needed to compress the toroidal field (paramagnetic effect) is lost. This energy is $\frac{1}{2}L_i I_p^2$, where I_p is the toroidal plasma current, L_i is the internal self-inductance, and the expression is evaluated at the end of the burn time. We introduce a loss factor γ as an input parameter, by assuming the actual loss to be $\gamma \times \frac{1}{2}L_i I_p^2$. Since a fraction η_{th} of the dissipated field- and plasma energies can be recovered at the extinction of the plasma, the maximum value ($\gamma = 0.5$) has been taken.
In the earlier calculation of a screw-pinch reactor with circular cross-section [1,3] the last mentioned loss was not included, neither were the losses in the transmission systems; therefore the net efficiency found there was too optimistic. Free input parameters for the reactor calculation are the initial filling pressure, the initial bias field,

the temperature at the end of the compression stage, and the magnetic field at the start of the second burning stage. These are iterated to give a minimum capital cost per unit electrical output of the reactor. Other losses than described are either assumed to be negligible or taken into account by the value of the thermal efficiency.

4.2. Results and Discussion

Table 1 summarizes some important input and output parameters of the Reference Belt Screw-Pinch Reactor (BSPR). An impression of the capital costs is given in table 3.

Figure 5 shows the variation of some important reactor parameters with the input parameters A, P_w, P_{th}, η_{ets}, $\hat{E}_{wm}$, β, d_t, e, λ, and q. From these and other results it can be concluded that:

- an aspect ratio of A = 4 is a reasonable compromise between plasma equilibrium requirements and technology;
- the average total wall loading P_w is optimal at 2 MW/m^2; above this value the filling density would rise and the implosion temperature would fall, while below it the energy of the implosion bank would become too large;
- an increase of the thermal power above 6 GW would give some increase in efficiency, at 2.5 GW it would be zero;
- the ETS-system is less critical than in ref. [3], at $\eta_{ets} = 65\%$ the net efficiency would be zero;
- $\hat{E}_{wm}$ should be high, 3 kV/cm is taken as a technical limit. The external inductance of the implosion circuit must be kept low in order to limit the bank energy and to reach $\hat{E}_{wm}$ during the implosion;
- β is still important, but values above 0.5 seem unrealistic;
- the thickness of the TF compression coils is approximately optimal at 2 m. For thicker coils the investments in coil materials and extra ETS-energy increase more than the efficiency. This is partly due to a weaker coupling between the PF-coil and the plasma at thicker TF-coils;
- an ellipticity e = 3 at the first wall gives e > 6 at the plasma boundary. It seems that due to augmented coil losses higher values of e (in order to achieve a higher β) would not be profitable;
- lower values of L_{ext}/L_{int} are profitable with respect to W_i, but engineering sets a limit to the value of L_{ext};

. higher values of q lower the contribution of the PF-coils to the ETS-energy and the ohmic losses;
. the burnup (30%) is high, but does not affect the reactor efficiency strongly;
. the parameters of the BSPR are not very sensitive to a change in costs of the different reactor components.

4.3. Cost Evaluation

A costs evaluation for the BSPR reference reactor has been performed based on unit cost estimates, derived from other system studies, e.g. |12|. The results are given in table 3. The unit costs of the homopolar generators are high, but in agreement with recent estimates |13|.
The unit costs of the capacitors are those for the present available (but slow) capacitor storage systems. The unit costs of the blanket include also the primary heat transfer system. The conventional plant includes the turbine plant, the 2500 MW_e electrical plant, and the civil structures.
The estimated total direct costs of the Reference BSPR are 3350 $/kW$_e$. For comparison: the direct costs of Tokamak power plants vary from 1000 to 2000 $/kW$_e$ |12|.
Following the cost procedures of reference |12|, which are based on extensive experience of the nuclear industry, the additional cumulative indirect costs and interest during construction are about 1.5 times the direct costs, so the total capital investments are 2.5 times as high as the direct costs of the components.
The total capital costs of the Reference BSPR then will be 8300 $/kW$_e$ compared to 2500 - 5000 $/kW$_e$ for Tokamak power plants. The calculated values are based on prices of 1977.
The energy storage system determines the costs of the BSPR for a large extent.
The non-conventional part (including the ETS) contributes for about 80% to the total plant costs.

5. BASIC CONSIDERATIONS ON SUPERCONDUCTING COILS FOR THE BSPR

The large ohmic losses in normally conducting copper coils have a detrimental impact on the net efficiency of the BSPR.
Application of superconducting coils, which under stationary conditions are practically free of losses, might lead to an increase of the total efficiency. Therefore, the consequences connected with the use of super-conducting coils have been considered for the case of a pulsed reactor.

The superconducting TF coils would have to generate a central peak field of 4.6 Tesla with a rise time not longer than 0.1 seconds, whereas the maximum field at the windings will be 8 Tesla. The maximum voltage supply is limited by the output of the homopolar machines and is as high as 8 kV. This restricts the number of windings of a coil to only one, this winding should then carry a total current of 10 MA. The space available for the normal coils is adequate to replace those coils by superconducting coils including support structures.
The superconducting coils, including insulation and reinforcement materials, will have a cross-section of 1 m^2 and the weight of one coil is about 200 tons.
Each of the 24 coils is thought to accommodate 1000 parallel subsections, electrically insulated and carrying 10 kA each. The cooling of each subsection can be provided by supercritical helium flowing through a central channel or through a number of separate channels with a cross-section of about 30% of the subsection. The copper-superconductor ratio can exceed 20 in this case.

The use of superconducting coils for pulsed fields gives rise to a considerable heat dissipation due to four different mechanisms:

1. Coupling losses during the periods of transient operation of the magnets.
2. Relaxation effects due to non-instantaneous homogenization of the current in the superconducting composite during energizing and de-energizing of the magnet.
3. Losses due to non-perfect transposition of the parallel subsections in the coil.
4. Heat inleak through the current leads from room temperature to 4.2 K and ohmic losses in the leads.

- Coupling losses are due to inductive normal cross-over currents through the matrix between the filaments. They depend mainly on the field rise per unit of time and the absolute value of the field. These losses can be minimized by twisting the entire conductor and by incorporating resistive layers around the filaments. The losses are still a subject of extensive research and optimization. Extrapolation from present data at 1.4 T/s of optimal 10 kA cables |14| to the estimated average pulse fields of 50 T/s for the present design leads to a heat dissipation of 500 kW at 4.2 K for the 24 coils together.

- Assuming for the moment that perfect transposition, such that all parallel subsections have exactly the same selfinductance, is technically achievable, the losses due to a normal current in the matrix, which occurs as long as magnetic flux penetrates into the composite, can be estimated.
  In the case of a 3×3 cm^2 subsection, with superconducting filaments equally distributed over a copper matrix and with a central cooling channel of 3 cm^2, the relaxation time for flux penetration can be estimated at 0.3 seconds.
  The heat dissipation due to relaxation losses with respect to the cycle time of 26 seconds is then about 600 kW at 4.2 K for the 24 coils.

- It will be technically very difficult to achieve a perfect transposition. Even a deviation of 1% in self-inductance from the ideal situation will cause a heat dissipation of the order of 10^{-5} of the stored magnetic energy in the coil windings. This results in an average heat dissipation of 400 kW for the total system. In practice even a transposition better than 1% will be hard to obtain. It is by no means certain whether this kind of heat dissipation can be kept lower than those in the two preceding paragraphs.

- Based on ref. |15|, it is possible to estimate the required cooling capacity for optimized current leads. A helium flow of at least 0.5 kg/s has to be supplied at low temperatures to each current lead if one allows the helium to heat up to room temperature.
  As a consequence, a mass flow of 24 kg/s of cold helium is required for the 24 pairs of current leads. This flow does not exceed the

amount of off-gas (75 kg/s) due to the losses mentioned earlier. Consequently this off-gas can be used for cooling the leads.

The type of superconducting material has not been specified until now. NbTi cannot be considered as an attractive candidate material. Although being cheap, having a high workability and having a good stability if clad with copper, the low critical temperature (6.2 K at 8 T) makes the stability margin under pulsed conditions very narrow. Nb_3Sn is a possible alternative (T_c = 14.3 K at 8 T) but it has a poor workability and it is expensive. A-15 conductors to which group Nb_3Sn belongs, are at present a subject of very extensive research and it is by no means possible to anticipate on the future economical and technical possibilities offered by this type of new conductors.

The total heat dissipated within the coils is estimated at 1500 kW. Taking into account a helium refrigeration efficiency of 1:300 for advanced systems with heat rejection at a temperature of 300 K |16|, a total electric power supply of about 450 MW will be required to keep the superconductor below its critical temperature. This power is about half of the ohmic losses in the normal conducting coils of the reference reactor. The net electric output of the reactor with superconducting coils therefore will be about 1.5 GWe (η = 25%) compared to 1.1 GWe for the reference reactor with normal coils. This improvement of the net efficiency is determined by the transposition and the relaxation loss. These may be higher in the real coil composition.

The weight of the superconducting coils will be about half the weight of the normal coils. Even if the superconducting coil costs are not higher than the costs for the normal coils themselves, the following important cost increasing factors have to be considered:

- In order to reduce the neutron and gamma heating in the superconducting coils (to avoid additional refrigeration capacity) extra shielding between blanket and coils has to be provided. This requires additional investments. Moreover, the inner diameter of the coils - and hence the total weight - will increase.
- The refrigeration system, with a power supply of 450 MW for 1500 kW heat dissipation being one or two orders of magnitude larger than for comparable Tokamaks, will cost about 100 M$ or more, and certainly will have a large impact on investment and space.

6. THE BSPR WITH FUEL INJECTION

6.1. General concept of fuel injection

In the reactor model described so far, the plasma is fuelled only between pulses. The efficiency of the resulting reference reactor is poor, partly because the high beta values reached relate only to the small fraction of the plasma vessel utilized by the reacting plasma. The reacting volume could be enlarged by fuel injection; outer shells of freshly provided fuel could gradually be ignited, or the fuel could be injected right into the plasma volume if this would expand in a way controlled by mild instabilities.

The reactor - designed for a given output - would be started with a lower initial filling density, requiring less energy for implosion, compression and confinement, and resulting in lower investments than for the reference reactor. Fusion energy could be used to ignite the added fuel. The expanding plasma would then fill a substantial part of the available volume, thus increasing the average beta.

There is no information on the plasma stability in a screw pinch that is refuelled. With the assumption that the plasma keeps itself at the stability limit for β, a study was started on the feasibility of injecting fuel pellets into the central plasma during a pulse without ash removal. The parameter study indicates that a net efficiency of about 30% may be reached, while (relative to the reference case) the magnetic field strength and the copper weight of the coils may be reduced by a factor of 2, the ETS energy by a factor of 2.5, and the number of capacitor banks by a factor of at least 10. The initial filling density of the plasma vessel is thereby assumed to be reduced by a factor of 10.

As a result the total capital investments are reduced by a factor of 1.5 and the relative capital costs ($/kW$_e$) by a factor of 2.4.

Table 4 summarizes the important parameters of the BSPR with fuel injection. Some details of the requirements for and the technological consequences of pellet injection are discussed below.

6.2. Technological consequences of pellet injection

The BSPR in this mode has a burn-up of 13% and needs a fuel amount of 4.75 g DT mixture per burn cycle.
Starting each cycle with the compression and ignition of a plasma with an initial fuel content of 100 mg, which is 10% of the nominal value for the reference reactor, a fuel amount of about 4.5 gram DT has to be injected during the first part of each burn phase.
To avoid a substantial cooling or even extinction of the initially ignited plasma the period over which the injection takes place has to be several seconds. Cluster injection |17| and neutral beam injection are unfavourable compared to pellet injection due to a high circulating power needed, and therefore are not considered here.
In our study the implications of the consecutive injection of several hundreds solid DT pellets of the order of 10 mg each have been examined in more detail. The mass of each pellet is low compared to the initial fuel present in the plasma torus (~ 100 mg), so minimum disturbances of the reacting plasma are expected. The implications of other pellet masses are also incorporated in the study.

The required velocity of the pellet depends not only on the need of a sufficient penetration into the reacting plasma but, to a greater extent, on the requirement that the pellets have to pass the not-ignited layers of the plasma without appreciable ablation.
Especially the transition region between the force-free outer layer (with low temperature and low density) and the burning plasma (with high temperature and high density) turns out to be decisive.

For refuelling the burning plasma, the freshly provided fuel might - from the plasma physics point of view - be deposited in the outer as well as in the inner shells of the burning plasma. Therefore, no special upper and lower limits seem to be required for the depth of penetration into the burning plasma.
The temperature and the density in the non-reacting force-free outer layer ($T_e \approx 0.5$ keV, $n_e \approx 10^{18}$-10^{19} m^{-3}) are one to two orders of magnitude lower than in the burning plasma region ($T_b \approx 7$ keV, $n_b \approx 5\times10^{20} m^{-3}$). In our calculations the temperature and density are assumed to increase linearly in the transition region. The thickness of this transition region is estimated to be one to two times the Larmor radius

of the 3.5 MeV fusion α-particles. For a magnetic field strength of 2.5 T this Larmor radius is ≈ 21 cm, and the transition region is taken to be about 30 cm.

During the ignition phase of the plasma the temperature in the outer region increases to several hundred eV by Joule heating. A subsequent increase of the density of this layer due to pellet ablation, up to a factor of ten might be allowed, without causing too much current dissipation, which would influence the plasma stability.

An estimate of the cooling by pellet ablation and Joule heating results in an equilibrium temperature of about 0.5 keV.

For our fuel scheme of 4.5 g fuel supply this gives a maximum allowable mass loss in the force-free outer layer of 4% of the initial pellet mass.

In view of the relatively low temperatures in the non-burning regions the calculations of the ablation rate and the lifetime of the pellets have been performed with the neutral-ablation, neutral-shield model, originally developed and verified at ORNL [18,19].

In this model the ablation rate $\dot{r}_p$ and the ablation time τ (i.e. the lifetime of the pellet in the plasma) scale as

$$\dot{r}_p \sim r_p^{-2/3} \, n_e^{1/3} \, T_e^{a}$$

and

$$\tau \sim r_p^{5/3} \, n_e^{-1/3} \, T_e^{-a}$$

in which r_p is the pellet radius, n_e is the plasma electron density, T_e is the plasma electron temperature, and a is an exponential factor varying from 1.64 to 1.84 depending on which specific ablation model is used.

The results of the calculations are as follows:

- The minimum velocity, v_{min}, of a 10 mg pellet ($r_p \approx 2$ mm) required to reach the burning plasma region is about 2500 m/s. This velocity is weakly dependent on the temperature level in the force-free outer layer. Also the minimum velocity is hardly affected by the specific ablation model used.
- For higher velocities more pellet mass is deposited in the burning plasma. A pellet with a velocity of 4 v_{min} will retain 60% of the initial pellet mass for refuelling the burning plasma. To retain more than 80% of the initial pellet mass a velocity in excess of 10 v_{min} is required.

- A 10 mg pellet with a velocity of 10^4 m/s will deposit about 60% of the initial pellet mass in the burning plasma. Such a pellet loses only a small fraction of its mass in the low density force-free outer layer (0.3% at 100 eV, 2.5% at 500 eV, and 8% at 1 keV).
  The penetration depth of the remaining pellet mass in the dense hot burning plasma is about 25 cm.
  In the calculations the ablated fuel mass in the transition zone is not considered as a loss; it is assumed to be taken up automatically by the burning plasma in the course of the plasma expansion.
- Pellets larger than the 10 mg considered are profitable with respect to the required velocity, pellet kinetic energy, and number of pellets. Taking the same constraints for the mass deposition in the successive layers and the same penetration depth in the plasma, the forementioned parameters scale as $v \sim r_p^{-5/3}$, $E_{pellet} \sim r_p^{-1/3}$, and $N \sim r_p^{-3}$.
  The maximum size of the pellets, however, will be limited by the influence of sudden local density and temperature disturbances on the stability behaviour of the burning plasma. In this respect and in view of the initial fuel mass of 100 mg, pellet masses should be kept within the range of several times 10 mg.
- In the ablation models used, magnetic and electrostatic shielding of the pellet are not taken into account. This shielding might increase the lifetime of the pellet and mitigate the velocity requirements.

This analysis shows that pellet velocities in the range $10^3 - 10^4$ m/s can satisfy the refuelling requirements of the BSPR which are less restrictive than for those Tokamak refuelling schemes, where pellets are thought to need higher velocities to penetrate far inside large hot plasmas.

Of the pellet acceleration systems mechanical, pneumatic, electrostatic, and laser acceleration systems have been examined [20-24]. Due to the low mechanical tensile strength of the solid DT ice pellets ($\sigma_{max} \approx 5\ 10^5$ N/m^2) and the low maximum allowable charge-to-mass ratio ($\approx 10^2$ C/kg for a 10 mg pellet) mechanical, pneumatic and electrostatic acceleration are less eligible. With a gas pressure of the same order as σ_{max}, the pneumatic system needs a tube length of about 100 m, but continuous operation is doubtful [22]. The electrostatic system needs maximum acceleration voltages >> 100 MV and maximum acceleration drift tubes > 1000 m [21] to accelerate 10 mg ice pellets up to 10^4 m/s.

Recent publications [23,24] suggest that creating ablation pressures with the objective to accelerate pellets up to 10^4 m/s could probably be achieved with existing laser technology. Assuming therefore that laser acceleration is the most promising acceleration scheme, the consequences of this system for the BSPR performance have been studied in some detail.

The kinetic energy of one 10 mg pellet with a velocity of 10^4 m/s is 500 J. Based on estimates of the efficiency of laser acceleration systems [23] and scaling laws derived from laser acceleration experiments [24], the nominal value of the energy supply to the laser gun is about 1 MJ per pellet. Laser systems of this capability are within technical realisation. The total efficiency of the acceleration system is low (<< 1%).

This total efficiency includes the efficiency of the laser, the efficiency of light absorption by the pellet, the fraction of absorbed light for ablation, and the propulsion efficiency of the ablated flow. Per burn cycle a total energy supply of ~ 450 MJ to the laser acceleration system is required. The electric energy produced in each burn cycle will be ~ 100 GJ so, in spite of the low efficiency, the power needed for the acceleration system has only a minor influence on the energy balance and the net efficiency of the reactor.

For the acceleration of a heavier pellet a more powerful laser gun is needed, because according to [24] the energy supply per pellet scales as $E_{gun} \sim r_p$. Pellets larger than 10 mg, therefore require stronger laser guns. Only with respect to the total energy supply of the acceleration system larger pellets are profitable (scaling as $\sim r_p^{-2}$) but as stated, the total installed power for the acceleration system is of such minor importance that this advantage is not decisive. In a further design optimization on pellet mass, mass distribution, and laser systems is needed.

For the present study a hundred identical multiple pulse laser guns distributed around the plasma vessel are supposed to accelerate the 450 pellets of 10 mg to be injected during each burn cycle. In case of lasers with higher repetition rate, this number could be reduced.

The investment costs for the injection system will be ~ 200 M$, and the power supply (~ 100 MJ of capacitors) will cost ~ 100 M$. These additional costs are much lower than the cost savings for the coil

structure and ETS system due to the lower magnetic field and magnetic energies needed in this reactor as compared to the reference BSPR, see table 5.

This analysis shows that the BSPR with pellet injection could be feasible. With its higher net efficiency, this reactor could be economically more competitive with Tokamak reactor plants.

A benign behaviour of the plasma to the fuel injection is, however, as yet not proven.

7. CONCLUSIONS

From the study the following conclusions are drawn:

1. The net efficiency and the investments of coils and storage systems of the belt screw-pinch reactor are improved compared to the screw-pinch reactor with circular cross-section.
2. The incorporation of more realistic estimates for the losses has caused the net efficiency to be low (for the corresponding circular reactor the net efficiency would even have been zero). This is caused mainly by the high ohmic and switching losses in the normal conducting coils. This again reflects the inefficient way of heating a plasma by adiabatic compression using resistive coils.
3. The limitations of large fast-switched capacitor banks at high voltages imply that the application of the implosion mechanism on a reactor scale will meet considerable difficulties.
4. The application of superconducting coils might somewhat improve the reactor efficiency but the considerable cost increase and the complex technological aspects connected with the fabrication of pulsed superconducting coils and its integration in the reactor system show that the use of pulsed superconducting coils is not a viable alternative for the BSPR.
5. A more promising alternative could be injection of fuel during the burn. This would result in an expansion of the burning plasma into a larger part of the plasma vessel, utilising the large β values. The same power output would then be reached with less investment and power input for implosion and compression. Although preliminary calculations look promising, such a scheme poses new problems in the domain of plasma physics.

REFERENCES

|1| Bobeldijk, C., et al., "Current decay and stability in SPICA", Proc. 6th Int. Conf. on Plasma Phys. and Contr. Nucl. Fusion Res., Berchtesgaden 1976, vol. I, p. 493.

|2| Bobeldijk, C., et al., "Parameter study of a screw-pinch reactor", Proc. 9th Symp. on Fusion Techn., Garmisch-Partenkirchen 1976, p. 367.

|3| Bustraan, M., et al., "Parameter study of a screw-pinch reactor with circular cross-section", ECN-16 (1977), also as Rijnhuizen Report 77-101.

|4| D'Ippolito, D.A., et al., "Maximizing β in a Tokamak with force-free currents", Proc. 6th Int. Conf. on Plasma Phys. and Contr. Nucl. Fusion Res., Berchtesgaden 1976, vol. I, p. 523.

|5| Hoekzema, J.A., Schuurman, W., "Parameter calculation of a screw-pinch reactor with elongated cross-section", Rijnhuizen Report 79-117, Jutphaas 1979.

|6| Verschuur, K.A., "Neutronics in the toroidal belt geometry of a screw-pinch reactor", Proc. 10th Symp. on Fusion Tech., Padua 1978 (paper G1).

|7| Abdou, M., "Wall load and lifetime goals for Tokamak power plants", Trans. ANS 27 (1977) 13.

|8| Rovner, L.H., Hopkins, G.R., "Ceramic materials for fusion", Nucl. Techn. 29 (1976) 274-302.

|9| Aronstein, R., Ghose, S.K., "Cost components of fusion power plants", Trans. ANS 26 (1977) 45.

|10| Thomassen, K.I., "Conceptual engineering design of a one-GJ fast discharging homopolar machine", EPRI-ER-246 (1976).

|11| Hoekzema, J.A., et al., "Heating of a pinch at intermediate β-values", Rijnhuizen Report 76-98, Jutphaas 1976.

|12| Badger, B., et al., "UWMAK-III, A noncircular Tokamak Power Reactor Design", UWFDM-150, Wisconsin, 1976.

|13| Thomassen, K.I., "Fusion applications of fast discharging homopolar machines", EPRI-ER-625 (1978).

|14| Kwasnitza, K. and Horvath, I., "AC losses of cabled and soldered multifilament super-conductors designed for large current", document published by the Institute of Solid State Physics ETH, Zürich and Boveri & Co. Ltd., Zürich.

|15| Scott, J.P., "Current leads for use in liquid helium cryostats", Proceedings ICEC 3, Berlin, 1970 (IPC 1970).

|16| Strobridge, T.R., "Feasibility study of a multipurpose refrigerator for a superconducting cable test facility", EPRI-282, July 1975.

|17| Bottiglioni, F. et al., "Cluster beam injection", EUR-CEA-FC-931, November 1977.

|18| Milora, S.L. and Foster, C.A., "ORNL Neutral Gas Shielding Model for Pellet-Plasma Interactions", ORNL-TM-5776, May 1977.

|19| Parks, P.B. and Thurnball, R.J., "Effect of Transonic Flow in the Ablation Cloud on the Lifetime of a Solid Hydrogen Pellet in a Plasma", Phys. Fluids 21 (1978) 1735-1741.

|20| Dimock, D. et al., "Pellet acceleration studies relating to the refuelling of a steady-state fusion reactor", Risø-332, Nov. 1975.

|21| Lengyel, L.L. and Riedmüller, W., "Estimates on the Acceleration of Pellets by Gasdynamic and Electrostatic Means", IPP-4/171, Garching, July 1978.

|22| Proceedings of the Fusion Fueling Workshop. Princeton University, 1-3 November 1977, CONF-771129.

|23| Felber, F.S., "Laser Acceleration of Reactor-Fuel Pellets", Nuclear Fusion 18 (1978) 10, 1469-1471.

|24| Burgess, M.D. et al., "Acceleration of Macroparticles by Laser-light", CLM-P546, Culham, June 1978.

Table 1. Parameters of the Reference Belt Screw-Pinch Reactor (BSPR)

Input parameters		Output parameters	
aspect ratio	$A = 4$	half-width of the torus	$b = 2.5$ m
maximum β	$\beta_{max} = 0.5$	half-height of the torus	$h = 7.5$ m
thermal output power	$P_{th} = 6$ GW	large radius of the torus	$R = 10$ m
average wall loading	$P_w = 2$ MW/m^2	implosion energy	$W_i = 940$ MJ
max. E-field at wall	$\hat{E}_{wm} = 3\times10^5$ V/m	adiabatic compression energy	$W_a = 111$ GJ
thermal efficiency	$\eta_{th} = 0.42$	burn time	$t_b = 18$ s
ETS efficiency	$\eta_{ets} = 0.95$	cycle time	$t_c = 26$ s
torus elongation	$e = 3$	burnup	31.6%
blanket thickness	$d_b = 0.8$ m	filling density	$n_o = 7\times10^{19}$m^{-3}
thickness TF coils	$d_t = 2$ m	bias field	$B_o = 0.2$ T
safety factor at wall	$q = 2$	B after implosion	$B_{eq} = 0.5$ T
filling factor Cu-coils	$f_c = 0.7$	B after compression	$B_a = 4.6$ T
energy multiplication of the blanket	$Q_m = 1.2$	mean B during the burn	$\overline{B} = 3.6$ T
		T after implosion	$T_{eq} = 1.25$ keV
		mean T during the burn	$\overline{T} = 9$ keV
		rel. plasma volume after compression	$V = 0.05$
		net electric output	$P_{net} = 1.12$ GW
		net efficiency	$\eta_{net} = 18.7\%$

Table 2. First-Wall Loading and Power Distribution in the BSPR.

	Outer blanket	Inner blanket	Upper+lower blanket	Total reactor
First-wall area (m^2)	1175	700	625	2500
% of first-wall area	47	28	25	100
First-wall loading (MW/m^2)				
maximum	5.3	3.1	1.7	5.3
minimum	0.75	0.42	1.10	0.42
average	2.6	1.6	1.5	2
% of total first-wall loading	59.9	22.1	18.0	100
Power production (GW_t)	3.29	1.40	1.32	6
Power production in MW per m^2 first-wall area				
maximum	5.4	3.4	2.3	5.4
minimum	1.12	0.85	1.6	0.85
average	2.8	2.0	2.1	2.4
% of total power production	54.7	23.3	22.0	100

The wall loading includes the neutron wall loading and the heat load from the plasma.

Table 3. Economic Parameters of Reference Belt Screw-Pinch Reactor (BSPR)

	volume (m^3)	weight (tons)	unit cost estimate	capital cost estimate
blanket	2000		165 k\$/m^3	330 M\$
TF coils	4250	27000	20 \$/kg	540 M\$
PF coils	1820	11000	20 \$/kg	220 M\$
transmission lines	1500	9000	20 \$/kg	180 M\$
implosion banks (940 MJ)	24000	20000	0.5 \$/J	470 M\$
ETS (111 GJ)			0.01 \$/J	1110 M\$
conventional plant	(6000 MW_{th}/2400 MW_{gross})		150 \$/kW_{th}	900 M\$
		Total direct costs		3750 M\$
		Relative direct costs		c = 3350 \$/kW_e
		Total copper weight		G = 47 ktons
		Relative copper weight		g = 42 kg/kW_e
		Total relative capital costs		8300 \$/kW_e

Table 4. Parameters of the BSPR with fuel injection.

(Only the parameters different from those of the reference reactor are given).

thickness TF coil	d_t = 1 m
implosion energy	W_i = 70 MJ
adiabatic compression energy	W_a = 45 GJ
max. E-field at wall	$\hat{E}_w$ = 0.4 10^5 V/m
burn time	t_b = 27 s
cycle time	t_c = 41 s
filling density	n_o = 7x10^{18} m^{-3}
bias field	B_o = 0.04 T
B after implosion	B_{eq} = 0.12 T
B after compression	B_a = 2.4 T
T after implosion	T_{eq} = 0.7 keV
mean T during burn	T = 7 keV
relative plasma volume after compression	V_1 = 0.018
relative plasma volume after pellet injection	V_2 = 0.49
burnup	13%
net electric output	P_{net} = 1800 MW_e
net efficiency	η_{net} = 30%

Table 5. Economic parameters of the BSPR with pellet injection

	Volume (m^3)	Weight (tons)	Capital cost estimate (M$)
blanket	2000		330
TF coils	2100	13000	260
PF coils	910	5500	110
transmission lines	750	4500	90
implosion bank (70 MJ)	2000	1600	35
ETS (45 GJ)			450
conventional plant ($6000\ MW_{th}/2400\ MW_{gross}$)			900
pellet acceleration system			200
pellet acc. power supply			100
Total direct costs			2475 M$
Relative direct costs			1375 $/$kW_e$

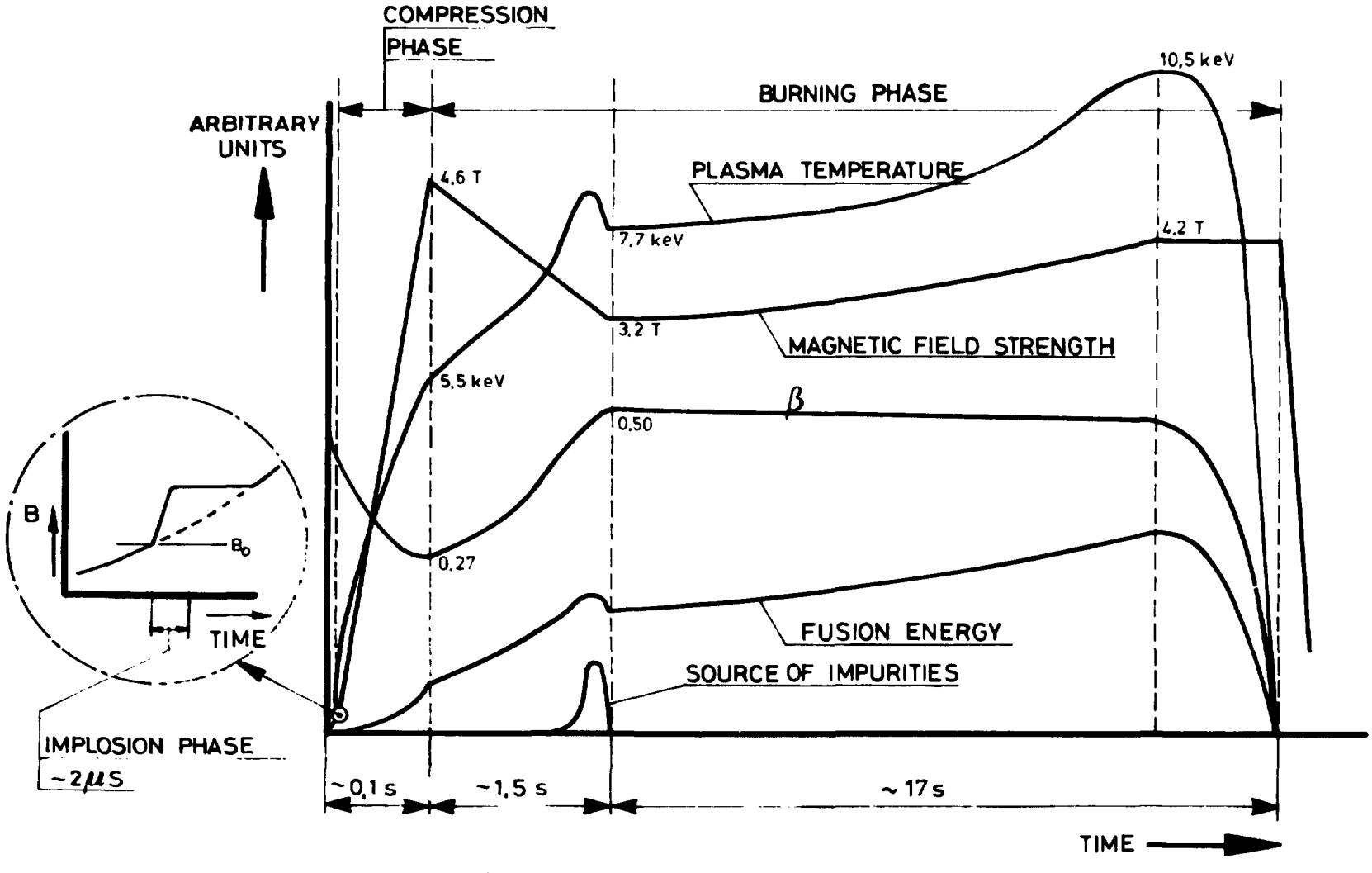

Fig. 2. Time dependence of the magnetic field strength, the temperature, the value of β, the produced fusion energy, and the number of injected impurity atoms.

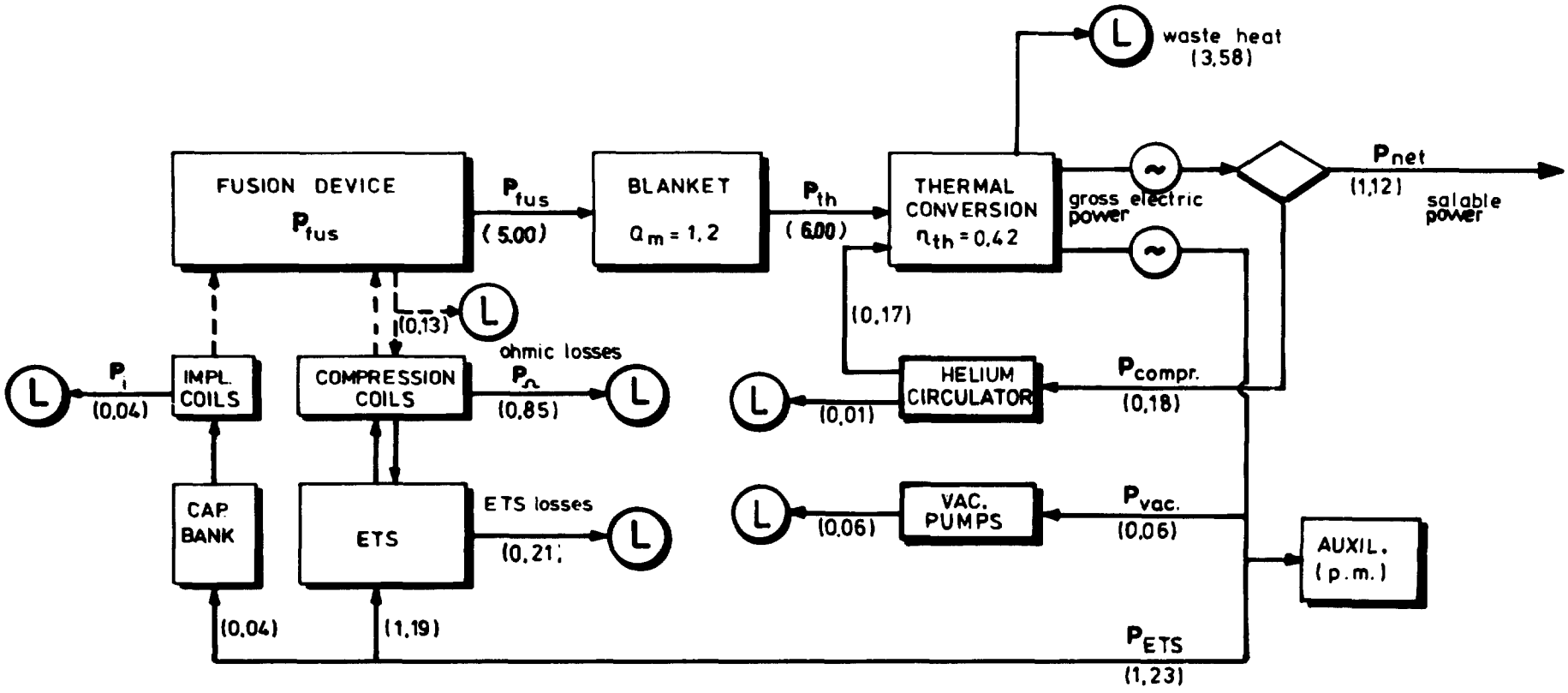

Fig. 3. Energy-flow diagram of the BSPR, data are given for the reference case in GW.

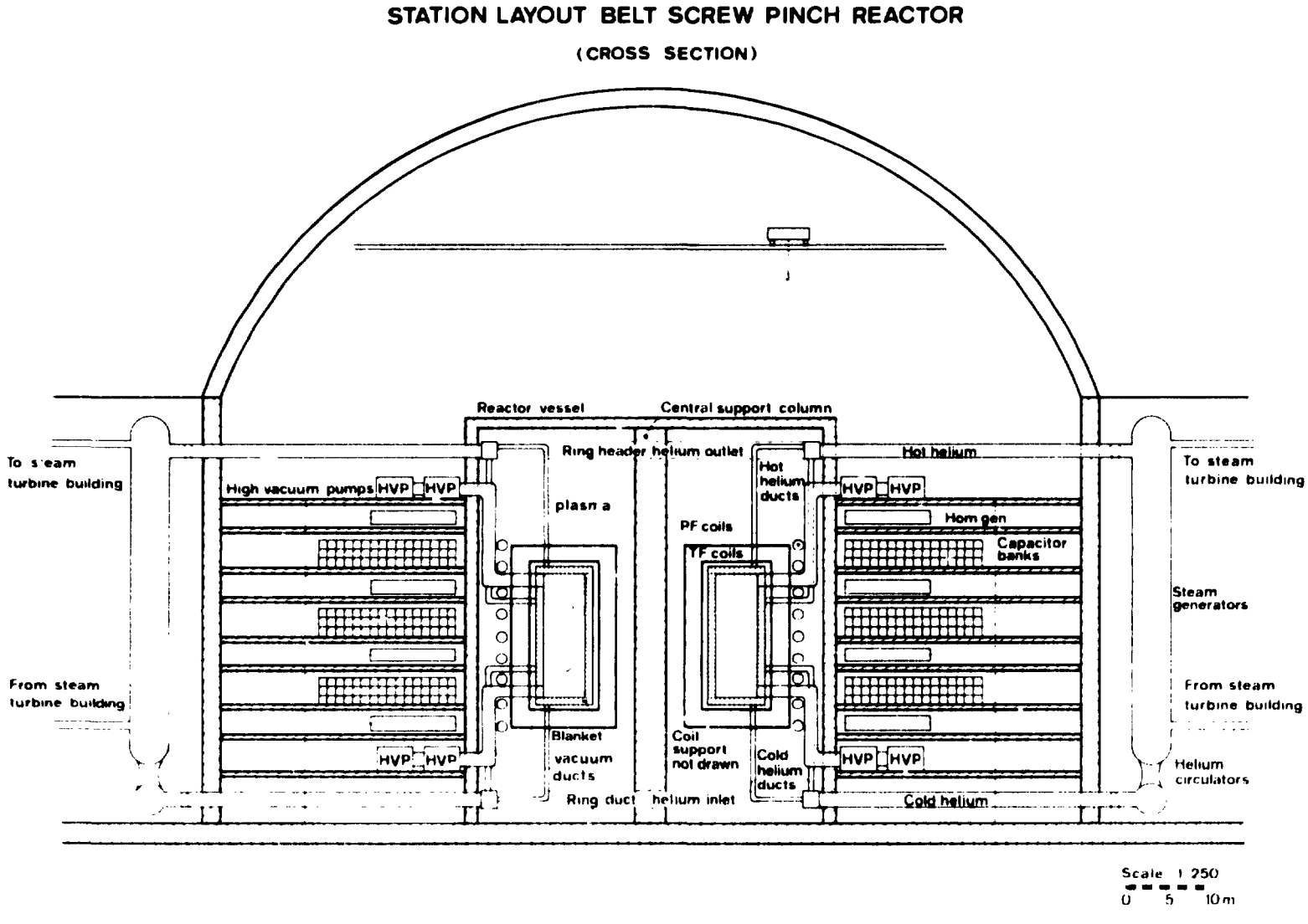

Fig. 4a. Station lay-out of the BSPR, vertical cross-section.

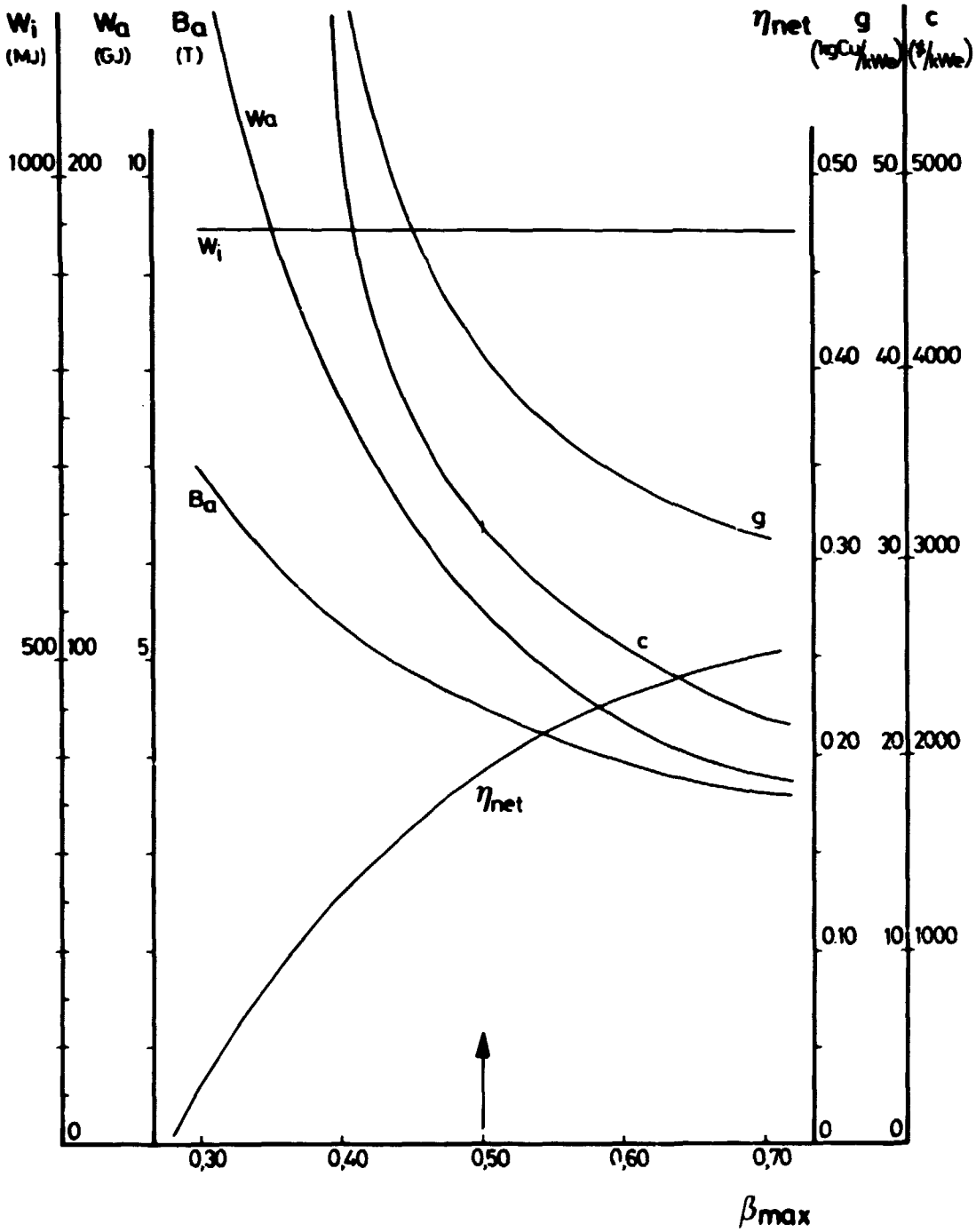

Fig. 6d. (continued)

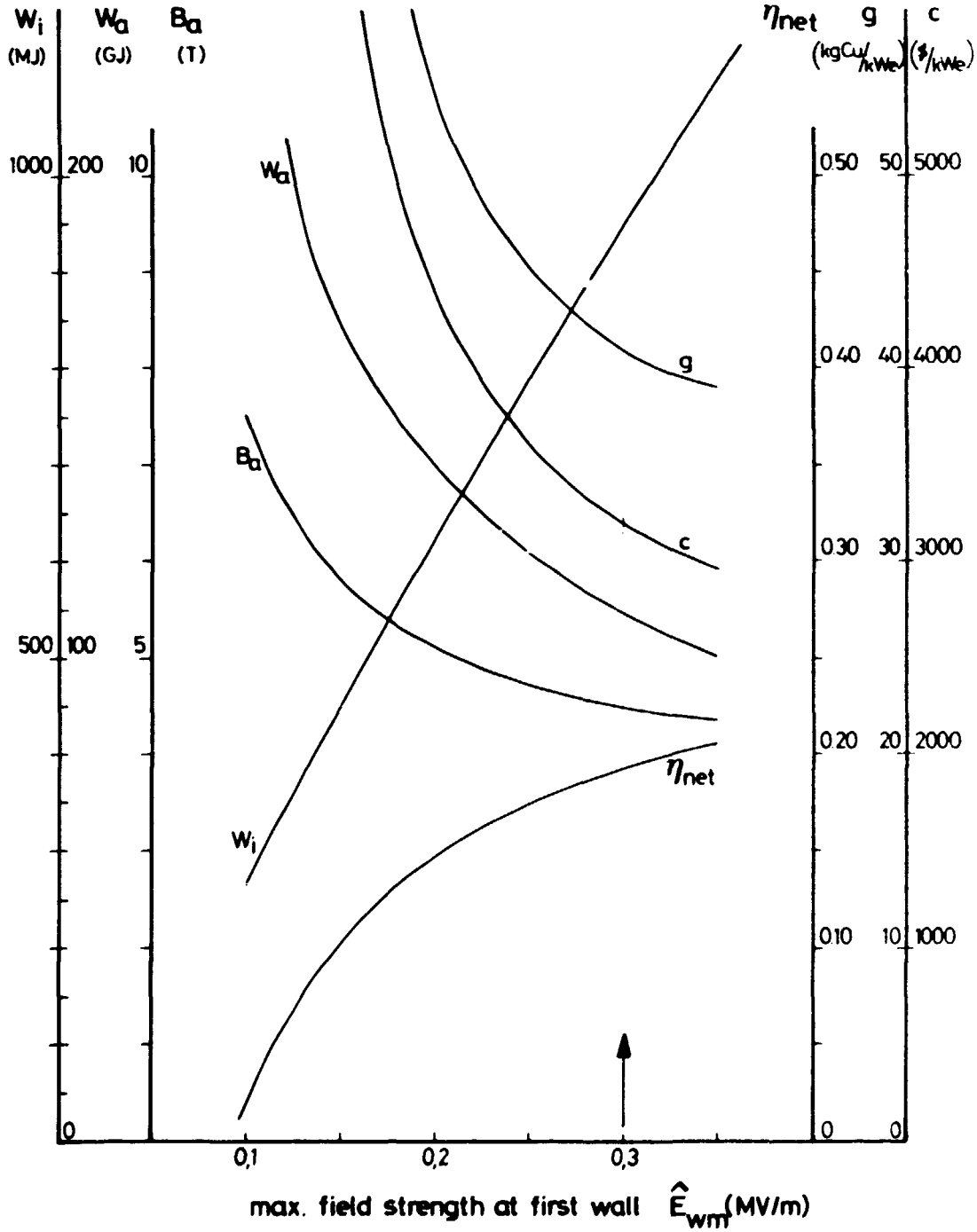

Fig. 6f. (continued)

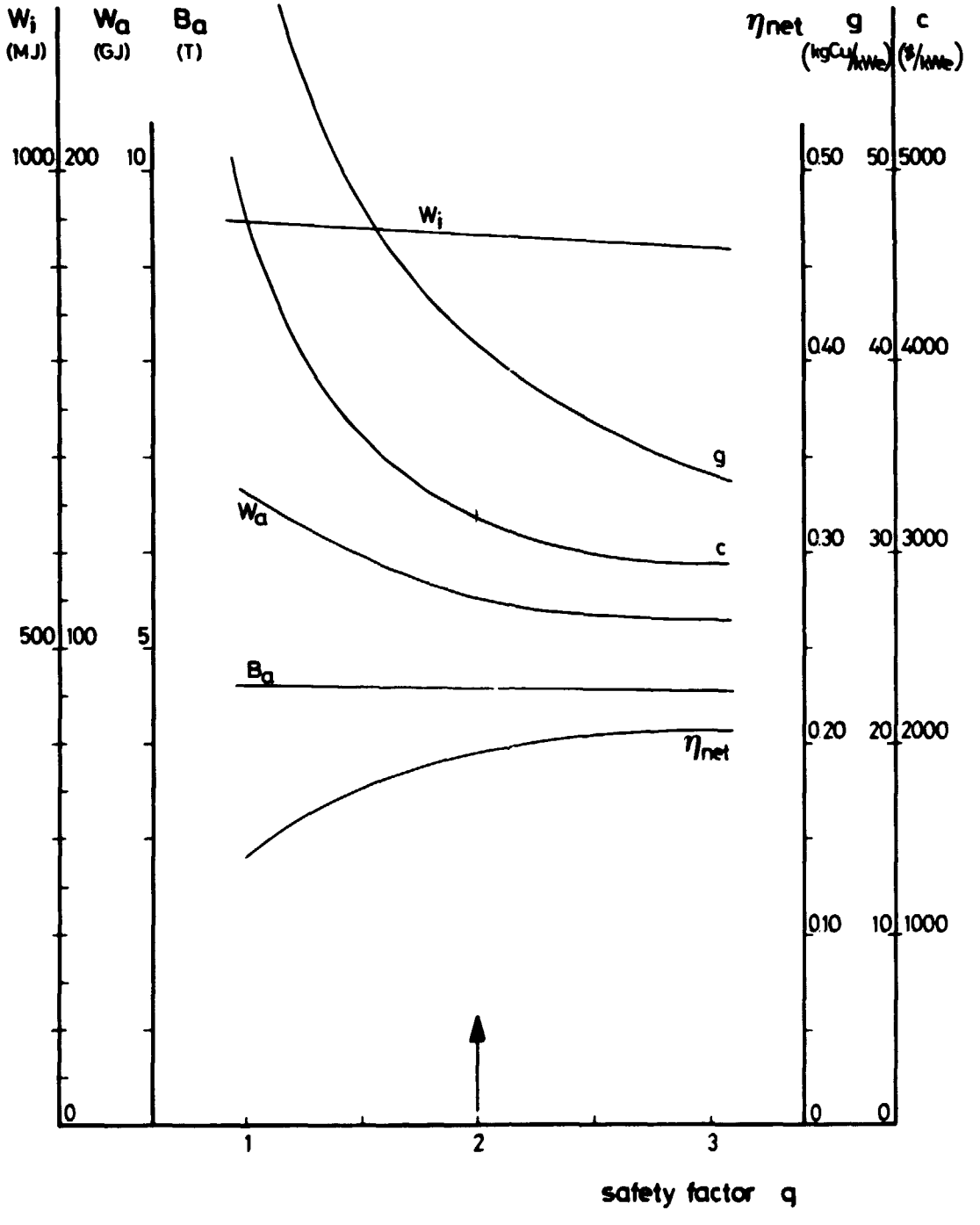

Fig. 6j. (continued)